2017 2nd International Conference on Industrial Aerodynamics (ICIA 2017)
ISBN: 978-1-60595-481-3

Aerodynamic Performance of Trains with Different Longitudinal Section Lines under Crosswind

Taizhong Xie and Tanghong Liu

ABSTRACT

Aerodynamic analysis of trains with different longitudinal section lines under crosswind was studied using the CFD methods in this paper. The slopes of five different longitudinal section lines are 0.58, 0.54, 0.5, 0.46, 0.42, respectively. The results show that the drag coefficient increases 27.6% and the lift force increases 12.3% with the slope of longitudinal section line increases from 0.42 to 0.58, but the lateral force varies little. The drag coefficient and lift force increase logarithmically with the slope of longitudinal section lines. With the increase of the slope of longitudinal section line, the surface pressure coefficient of the windward side is basically unchanged, but the surface pressure coefficient of the leeward side is decreasing. Comparing the flow field around the train, it is found that the longitudinal section line has no obvious influence on the flow field structure of the lead car, the vortex of the leeward of the middle car and the tail car increases with the slope of longitudinal section line increases.

Key word: Longitudinal section line; Crosswind; High-speed train; Aerodynamic

Taizhong Xie, Key Laboratory of Traffic Safety on Track of Ministry of Education, School of Traffic & Transportation Engineering, Central South University, 22 Shaoshan Road, Changsha, China.
Email: csuxtz@csu.edu.cn

1. INTRODUCTION

With the increase of train speed, the shape of the train on its aerodynamic performance is also increasingly important, especially in the crosswind, the drag force, lift force, and lateral force of the train will further increase[1]. Compared with the traditional blunt train, streamlined train can effectively reduce the drag and improve the stability under crosswind[2]. Because of the light weight of the high speed train, it has certain danger of overturning. In recent years, many experts and scholars have done a lot of research on the influence of parameters of train crosswind stability.

Baker[3] calculated the outflow field distribution of train under different train speed and different wind speed, the intuitive distribution of flow field is given. Hemida et al.[4] used LES method to study the flow fields around trains with different nose shapes. The results showed that the nose flow structure of short-nosed train is more unstable, and more vortex structures appeared in the tail. Liang et al.[5] optimized the aerodynamic shape of passenger train body under strong wind, and got the variation law of aerodynamic coefficients with wind speed. Wilemsen et al.[6] carried out the wind tunnel test, the influence of the train type, formation, operation speed, nasal tip shape and geomorphology of the vehicle on the aerodynamic characteristics of the vehicle was studied systematically.

Based on the above discussion, it can be found that there are many researches on the aerodynamic shape of the train and the aerodynamic performance of the trains under the crosswind. However, it is mainly aimed at the effect of nose length change of the train, wind speed and wind direction effect on the aerodynamic performance of the train. The influence of the main parameters of the train on the aerodynamic performance of the trains under the crosswind has not been studied in depth. Based on the above research, five different longitudinal section trains are designed, and the slope of longitudinal section line is 0.58, 0.54, 0.5, 0.46 and 0.42 respectively. The numerical simulation method is used to analyze the drag coefficient of different trains, the lift force and the lateral force are analyzed and compared in detail. The surface pressure distribution and the velocity field distribution around the train are also analyzed and discussed.

2. COMPUTATIONAL MODEL

The computational model is composed of three cars, including the lead car, the

middle car and the tail car, as shown in Figure 1. The length of the head car and the tail car is 25.7m, the middle car is 25m, and the total length of train is 76.4m. In order to facilitate modeling and calculation, the train omitted the handle, doors and windows and other fine structure, retaining inter-carriage gaps and bogies.

Figure 1. Computational model.

The streamlined length of the prototype train is 9m, and the slope of longitudinal section line is 0.5. On the basis of the prototype train, the longitudinal section line is changed, as shown in Figure 2 and Figure 3. The greater the slope of the longitudinal section line, the more convex the shape of the longitudinal section line. The Z0 stands for a prototype car. On the basis of the prototype car, the slope of the vertical profile is varied, and Z1, Z2, Z3 and Z4 are obtained. The slope of the longitudinal section line of five trains was 0.58, 0.54, 0.5, 0.46 and 0.42 respectively. The five train models have the same profile parameters except the slope of the longitudinal section line.

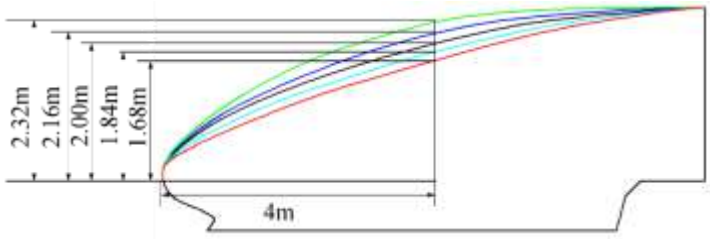

Figure 2. The different longitudinal section lines.

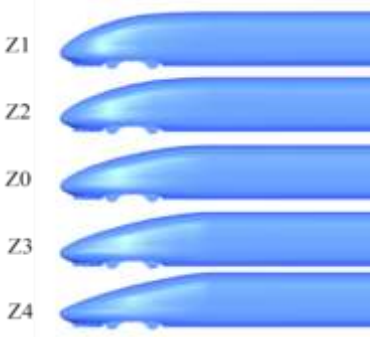

Figure 3. The different train models.

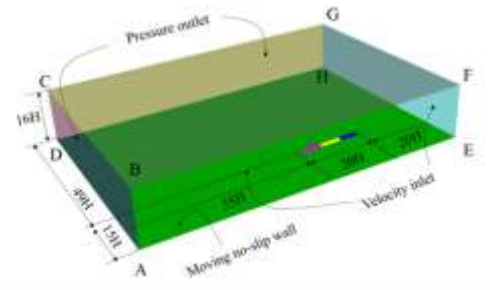

Figure 4. Computational domain.

3. COMPUTATIONAL DOMAIN AND MESH

The computational domain is shown in figure 4. A simplified 1/8-scale model is used in this paper. The height of train stands for train characteristic height, and the value is 0.38 m. The boundary is 20 H from the nose of the lead car and 55H from the nose of the tail car. The roof is 16H from the ground. The distance between the windward side and train is 15H and it is 49H between the leeward side and train. The face AEFB and EFGH are set as velocity inlet, and the speed of the train is 44.44m/s, the wind speed is 30m/s. The face ABCD and DHGC are specified as pressure outlet. The lower face AEHD is specified as a moving no-slip wall with a speed equal to the train velocity. The Re=1.7×10^6 based on the H and the synthetic speed of train and wind speed.

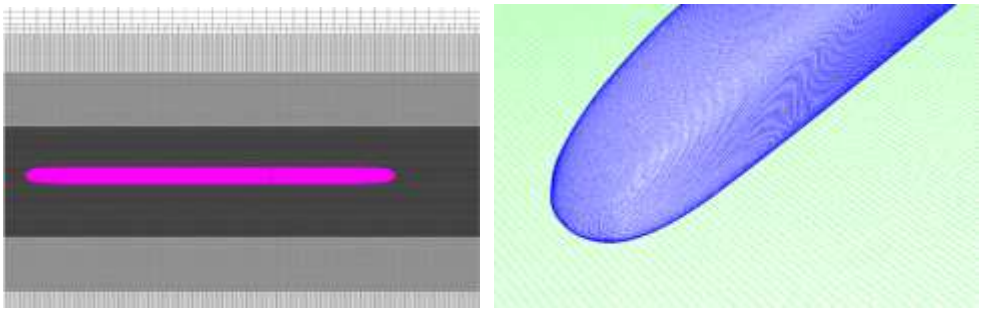

(a) mesh around the train (b) mesh on the surface of the lead car.

Figure 5. Computational mesh.

The mesh around the train is shown in Figure 5, the mesh is generated using SnappyHexMesh, a utility within OpenFOAM, and the mesh has 46 million cells in this study. In order to simulate the near wall flow of the train correctly, 10 prism layers cells are applied to the surface of the car, and the thickness of the first prism layer is 0.45mm, y+ of the most of the train surfaces is between 30 and 150 in this condition, which meets the calculation requirements.

4. VALIDATION

In order to verify the accuracy of aerodynamic drag calculation results, the experimental data of CRH2 wind tunnel test is used to verify. The test was carried out at the second test section of 8m×6m wind tunnel, China Aerodynamics Research and Development Center, as shown in Figure 6. A detailed description of the wind tunnel test is shown in reference[7]. In the wind tunnel experiment, the

wind speed is 60 m/s and the yaw angles are 0°, 10.22°, 15.14°, and 19.72°, respectively. In this paper, the yaw angle 0° is verified. CRH2 model use the calculation method of this paper for numerical simulation, and the calculation condition is the same as the wind tunnel test.

Table 1 shows the comparison results of wind tunnel experiment and numerical calculation, it can be seen that the difference of drag coefficient of the lead car is 4.73%, and that of the tail car is 2.45%, and the maximum difference is less than 5%. The numerical results are in good agreement with the wind tunnel test results.

Figure 6. The wind tunnel test.

TABLE 1. THE COMPARISON OF WIND TUNNEL EXPERIMENT AND NUMERICAL CALCULATION.

		Wind tunnel experiment	Numerical calculation	Difference
Drag coefficient	Lead car	0.148	0.141	4.73%
	Tail car	0.163	0.159	2.45%

5. RESULTS

5.1 Analysis of aerodyamic force

For ease of analysis, drag and surface pressure are expressed as dimensionless coefficients. The variation of the normalized pressure coefficient are defined as follow,

$$C_{\mathrm{d}} = \frac{F_{\mathrm{d}}}{0.5\rho u^2 A} \quad C_{\mathrm{l}} = \frac{F_{\mathrm{l}}}{0.5\rho u^2 A} \quad C_{\mathrm{h}} = \frac{F_{\mathrm{h}}}{0.5\rho u^2 A} \quad C_{\mathrm{s}} = \frac{F_{\mathrm{s}}}{0.5\rho u^2 A} \tag{1}$$

Where F_D represents the drag force, F_l represents the lift force,

F_h represents the lateral force, F_s represents the surface pressure, ρ represents the air density, which is 1.225 kg/m3 in this work, u represents the synthetic velocity, the value is 53.62m/s, A represents the reference area, considering the scaling model, the cross section area of the train 0.1755m^2 is used in this work.

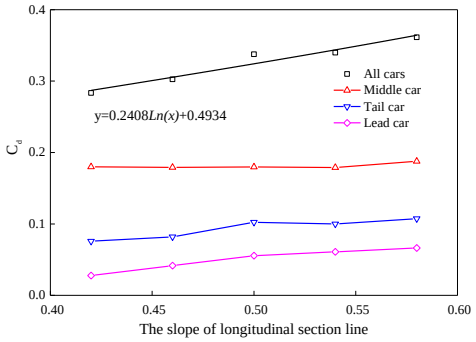

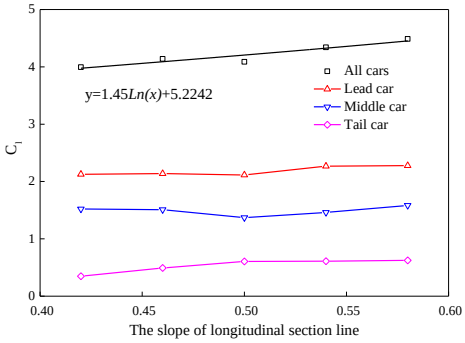

Figure 7. The drag coefficient of different trains. Figure 8. The lift force of different trains.

The drag coefficient is shown in Figure 7, the drag coefficient of middle car is the largest, and the drag coefficient of lead car is smallest. With the increase of slope of longitudinal section line, the drag coefficient of head, middle and tail cars shows an increasing trend. The total drag coefficient also increases with the slope of longitudinal section line, which is due to the obstacle of the head car to the airflow is stronger with the increase of the slope of longitudinal section line, and the pressure area increases. When the slope of longitudinal section line increased from 0.42 to 0.58, the total drag coefficient increased from 0.283 to 0.361, an increase of 27.6%. The total drag coefficient is logarithmically related to the slope of the longitudinal section line. The fitting formula is y = 0.2408Ln (x) +0.4934.

The lift force is shown in Figure 8, it can be seen that the lift is positive, which affects the stability of train operation. Unlike drag force, the lift force of lead car is the biggest, and the lift force of tail car is smallest. As the slope of the longitudinal section line increases, the lift force increases. When the slope of longitudinal section line increased from 0.42 to 0.58, the total lift force increased from 3.996 to 4.487, an increase of 12.3%. The total lift force is logarithmically related to the slope of the longitudinal section line. The fitting formula is y = 1.45Ln (x) +5.2242.

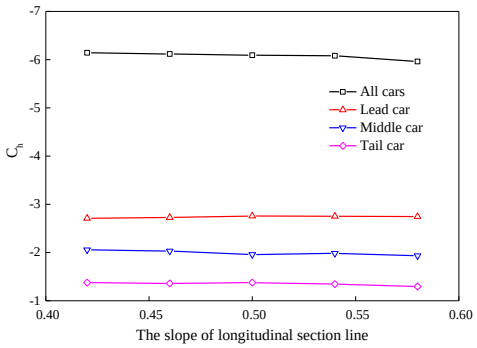

Figure 9. The lateral force of different trains.

The lateral force is shown in Figure 9, the lateral force of lead car is the biggest, and the lateral force of tail car is smallest. Unlike drag force and lift force, the lateral force is hardly affected by the slope of the longitudinal section line. When the slope of longitudinal section line increased from 0.42 to 0.58, the total lateral force only changed 2.7%, which is due to the change of the slope of the longitudinal section line has little effect on the change of the longitudinal section area, so the total lateral force is basically unchanged.

5.2 Analysis of surface pressure

In order to better analyze the surface pressure of the train, the corresponding measurement points are arranged on the surface of the train, and the middle car is used for the analysis. As shown in Figure 10, the number 43 to 51 is the measuring points of the windward side of the train, the number 52 to 54 is the top measuring points, the number 55 to 63 is the leeward side measuring points, and the number 64 to 66 is the measuring points at the bottom of the train.

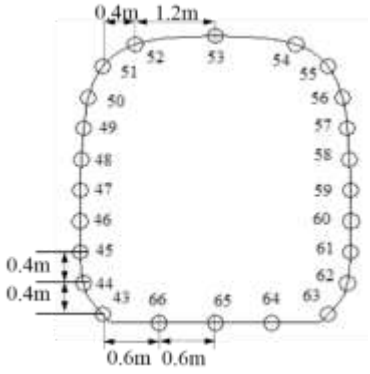

Figure 10. The measuring points of the middle car.

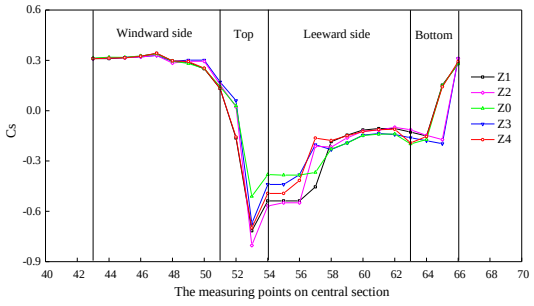

Figure 11. The surface pressure coefficient of intermediate section of different trains.

The variation curves of surface pressure coefficient of trains with different longitudinal section lines are shown in Figure 11, the variation rules of surface pressure coefficient of trains are consistent, the value is different due to the slope of the longitudinal section line is different. In the windward side region, the surface pressure coefficient of the train is positive and relatively stable. In the top region of the train, the surface pressure coefficient decreases rapidly and becomes negative, which is due to the airflow leads to a positive pressure zone at the windward side of the top of the train, and a negative pressure zone at the leeward side. In the leeward side of the train, the negative pressure gradually decreases and tends to be stable, and the pressure at the bottom of the train gradually increases to positive pressure. In the windward side, the surface pressure coefficient is basically unchanged with the slope increases. At the top of the train, the surface pressure coefficient decreases with the increase of the slope of the longitudinal section line. At the leeward side and the bottom of the train, the variation rule of the surface pressure coefficient is not obvious due to the field structure is complex.

5.3 Analysis of the flow around the train

The streamline diagram around the train section is shown in Figure 12, the pressure distribution of different longitudinal section line trains is basically the same, the windward side is mainly positive pressure and the leeward side is mainly negative pressure. The positive pressure area of the lead car is the largest and the positive pressure area of the tail car is the minimum, which leads to the lateral force of the lead car being relatively large. The more convex the longitudinal section line, the greater the positive pressure area in the windward side. For the leeward side, with the increase of the slope of longitudinal section line, the flow field around the lead car is basically unchanged. It is worth noting that, for the middle car and tail car, with the increase of the slope of the longitudinal section line, the vortex at leeward side increases from two to three, and the flow flied is more unstable, which indicates the increase of the slope of longitudinal section line has a greater influence on the leeward side of train, leading to greater risk of overturning.

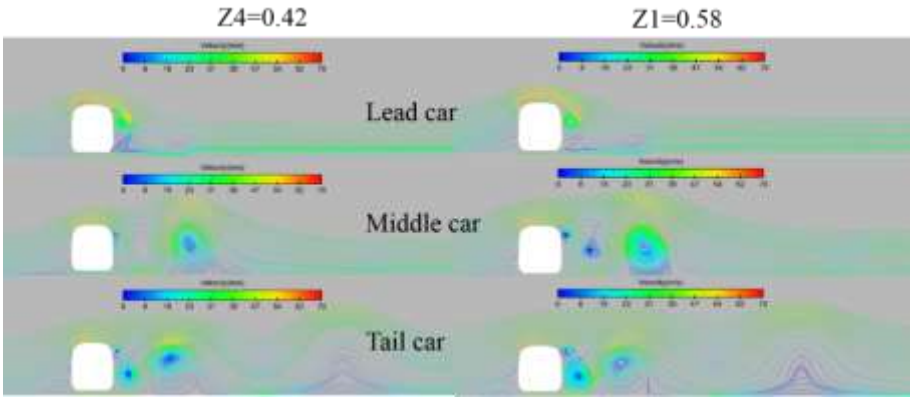

Figure 12. The streamline diagram around the train.

CONCLUSION

Five train models with different slopes of longitudinal section line are investigated using the CFD method in this work. Some conclusions are obtained as follows.

1. The drag coefficient and the lift force coefficient increase with the slope of longitudinal section line, and are logarithmic. The lateral force is almost unchanged with the increase of the slope of longitudinal section line.
2. The surface pressure coefficient of the top of train decreases with the increase of profile line. The surface pressure coefficient on the bottom and leeward side of the train is complicated and the law is not obvious.
3. With the increase of the slope of longitudinal section line, the number of vortices in the middle and tail car increases, and the flow field is more unstable than lead car.

ACKNOWLEDGMENTS

The computing resources were provided by the High-speed Research Center of Central South University, China. And this work was supported by the Technological Research and Development Program of China Railways Corporation (Grant No. 2016T004-E).

REFERENCES

1. Suzuki M, Tanemoto K, Maeda T. Aerodynamic characteristics of train/vehicles under cross winds[J]. Journal of Wind Engineering & Industrial Aerodynamics, 2003, 91(1):209-218.
2. Marzok C, Deh B, Courteille P W, et al. Crosswind stability of high-speed train on a high embankment[J]. Proceedings of the Institution of Mechanical Engineers Part F Journal of Rail & Rapid Transit, 2007, 221(2):205-225.
3. Baker C. The flow around high speed trains[J]. Journal of Wind Engineering & Industrial Aerodynamics, 2010, 98(6):277-298.
4. Hemida H, Krajnović S. LES study of the influence of the nose shape and yaw angles on flow structures around trains[J]. Journal of Wind Engineering & Industrial Aerodynamics, 2010, 98(1):34-46.
5. Jie Z, Liang X F, Liu T H, et al. Optimization research on aerodynamic shape of passenger car body with strong crosswind[J]. Journal of Central South University, 2011, 42(11):3578-3584.
6. Willemsen E. High Reynolds number wind tunnel experiments on trains[J]. Journal of Wind Engineering & Industrial Aerodynamics, 1997, 69(97):437-447.
7. Zhang Z, Zhou D. Wind tunnel experiment on aerodynamic characteristic of streamline head of high speed train with different head shapes[J]. Journal of Central South University (Science and Technology), 2013, 44(6):2603-2608.